Electronic and transport properties of single-wall carbon nanotubes encapsulating fullerene-based structures

D.-H. Kim, H.-S. Sim, and K. J. Chang
Department of Physics, Korea Advanced Institute of Science and Technology, Taejon 305-701, Korea
(Received 12 February 2001; published 24 August 2001)

We investigate the electronic and transport properties of (10,10) carbon nanotubes that contain a finite-sized capped (5,5) tube (capsule) and a long chain of C_{60} fullerenes by using the tight-binding model. We find that the total transmissions through the outer tubes are very sensitive to the symmetry of the hybrid tubes. For the (10,10) tube where the (5,5) capsule is aligned so as to maintain mirror symmetries, the total transmission exhibits antiresonances with symmetric line shapes, while breaking mirror symmetries leads to asymmetric line shapes. For encapsulated fullerenes in the (10,10) tube, we find rich structures in transmission, such as antiresonances, resonances, and transmission gaps, which depend on mirror and rotational symmetries. This feature is attributed to the fact that the coupling of incident channels with the bound states of the inner structures is determined by the symmetry of the hybrid tubes.

DOI: 10.1103/PhysRevB.64.115409 PACS number(s): 73.63.Fg, 71.20.Tx, 72.80.Rj, 73.61.Wp

I. INTRODUCTION

Carbon nanotubes (CNT's), which were discovered by Iijima,[1] have attracted great attention because of their unique electrical and mechanical properties, which are promising for nanodevices.[2] Many experiments have demonstrated the ballistic and coherent transport behavior of single-wall nanotubes (SWNT's), which exhibit resonant tunneling, quantum dot behavior, and standing waves in finite-sized tubes.[3–6] Because the phase relaxation length is larger than the typical tube length of a few micrometers, quantum interference effects are important in CNT's. Several theoretical attempts have been made to study the bound states of finite-sized CNT's,[7–9] and nanotube-based quantum dots.[10] Very recently, it has been suggested that antiresonances occur in transmissions through CNT's with polyhedral caps[11] and locally deformed regions.[12]

Recent experiments[13,14] have reported SWNT's encapsulating fullerene-based structures such as carbon nanotube capsules and fullerene chains. In these hybrid structures, closed carbon shells are contained within SWNT's with diameters of 1.3–1.4 nm. High-resolution transmission electron microscopy images indicated that many of these inner shells with diameter of 0.7 nm are fullerene molecules. Since inner molecules maintain the graphitic van der Waals spacing of 0.3 nm from the outer tube walls, these molecules interact weakly with the outer tube. Thus, interwall interactions may drastically alter the electronic and transport properties of surrounding SWNT's. In particular, in the coherent and ballistic transport regime, antiresonances are likely to occur on the geometrical analogy of nanotube wires with stub resonators.[15] In addition, since the electronic structure of SWNT's is determined by the arrangement of inner molecules, the transport properties are also affected by the geometry of hybrid structures. Despite many experimental observations of hybrid nanotube structures, there have been no comprehensive theoretical studies of the transport properties of these structures.

In this paper, we study the electronic and transport properties of single-wall (10,10) carbon nanotubes that contain a finite-sized (5,5) nanotube capsule and a chain of C_{60} molecules by using the tight-binding model and the Green's function approach. We investigate the effects of symmetries on the coupling of incident channels with the bound states of the inner structures and the total transmissions through the hybrid tubes. For the (5,5) capsule inside the tube, antiresonances generally occur in transmission, and are attributed to the increase of channels in the hybridized region. The line shape of these antiresonances depends on the alignment of the capsule; when mirror symmetries are maintained, Breit-Wigner-type symmetric line shapes are found, while breaking mirror symmetries leads to asymmetric line shapes. These features can be fully understood from the dependence of the antiresonance line shape on the reflection of incident channels and the wave vector difference between two channels in the hybridized region. On the other hand, for the (10,10) tube where C_{60} molecules are aligned so as to maintain both mirror and rotational symmetries, we find that antiresonance dips turn into resonancelike peaks as the number of molecules increases. If only mirror symmetries are broken, a transmission gap is developed, and resonance peaks occur in this transmission gap as rotational symmetries are further broken.

The paper is organized as follows. In Sec. II, we discuss the details of the hybrid tubes considered here and the calculational methods for the two-terminal conductances. In Sec. III, we derive a formula for the total transmission, and discuss the mechanism and characteristics of antiresonances in transmission, which help us to understand the transmission behavior in the hybrid tubes. In Sec. IV, the calculated total transmissions through (10,10) tubes that contain a finite-sized (5,5) tube and a chain of C_{60} molecules are given. Based on the band structures of the double-wall (5,5)-(10,10) tube and the (10,10) tube where C_{60} molecules are aligned periodically with various symmetries, we discuss the effect of symmetries on the total transmission. In Sec. V, a summary and conclusions are given.

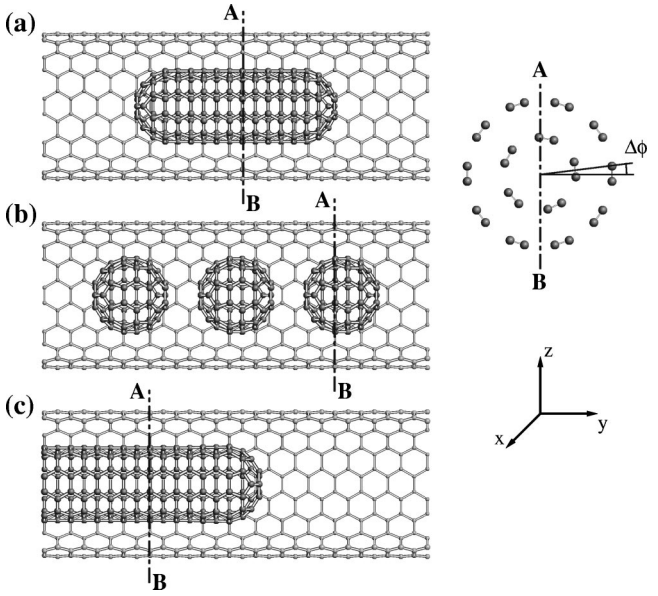

FIG. 1. The geometries and cross-sectional views of (10,10) tubes containing (a) a finite-sized (5,5) capsule, (b) a chain of C_{60} molecules, and (c) a semi-infinite capped (5,5) tube.

II. STRUCTURE AND CALCULATIONAL METHOD

To generate the hybrid nanotubes experimentally observed, we consider single-wall (10,10) tubes in which a finite-sized (5,5) capsule and a chain of C_{60} molecules are coaxially aligned, as shown in Fig. 1. We test various sizes for the (5,5) capsule and investigate the effect of mirror symmetries on transmission by rotating the capsule about the tube axis.[16] For the chain of C_{60} molecules, we vary the number of molecules, choosing the supercell geometry where a single molecule is contained in every four unit cells of the (10,10) tube. Thus, the distance between two neighboring C_{60} molecules is 1.0 nm, in good agreement with the measured value. When a fivefold rotational symmetry axis of C_{60} coincides with the (10,10) tube axis, we can break mirror symmetries only by rotating the molecule about the tube axis, while we maintain rotational symmetries. To break both mirror and rotational symmetries, we rotate the C_{60} molecule using Euler's angles about an arbitrary axis.

To calculate two-terminal conductances, we assume that inner structures are hybridized in a finite region of the (10,10) tube. Thus, unhybridized regions are used as input and output leads. The two-terminal conductance at zero temperature is obtained from the Landauer-Büttiker formula[17] $G=(2e^2/h)T(E)$, where $T(E)$ is the transmission of channels between the two leads at energy E. With use of the Green's function approach,[18] we calculate the transmission as a function of energy,

$$T(E)=\mathrm{tr}(tt^{\dagger})=\mathrm{tr}(\Gamma_L G^r \Gamma_R G^{r\dagger}), \tag{1}$$

where t is the transmission matrix and $\Gamma_{L(R)}$ is the coupling matrix between the left (right) lead and the hybridized region. Here G^r is the retarded Green's function in the hybridized region,

$$G^r=\frac{1}{E-H_d-\Sigma_L^r-\Sigma_R^r}, \tag{2}$$

where $\Sigma_{L(R)}^r$ is a self-energy and H_d is the Hamiltonian in the hybridized region, based on the tight-binding method.[19] We calculate Γ's and Σ's by employing the algorithm of López Sancho and co-workers.[20] The eigenchannels[21] are obtained by diagonalizing the 2×2 transmission matrix, which represents two channels near the Fermi level of the (10,10) tube. In this case, we can separate the total transmission $T(E)$ into $T_>$ and $T_<$, which correspond to more and less transmissive eigenchannels through the hybridized region, respectively, from the relations,[12]

$$\mathrm{tr}(T)=T_>+T_<, \tag{3}$$

$$\mathrm{tr}(T^2)=T_>^2+T_<^2. \tag{4}$$

The tight-binding method[19] is used to calculate the band structures of the hybrid tubes, assuming an infinite size for the inner shells. Although the hybridized regions are finite, these band structures are useful to understand the effects of interactions between the outer tubes and inner structures on the transport properties of incident channels.

III. ANTIRESONANCE

In semiconductor quantum wires with stub resonators, antiresonances are well understood using the *t*-stub geometry.[15] Although antiresonances are also expected in our hybrid nanotube systems, the *t*-stub geometry cannot be directly used because this model is too simple to describe wave propagation in the hybridized regions. Because of the coupling of inner structures with outer tubes, the number of channels in the hybridized region is not equal to that of the incident channels. If no channels exist in the hybridized region, incident waves are totally reflected, giving zero transmission. If the bound states in the hybridized region are weakly coupled with incident channels, the system becomes the well-known double-barrier problem, and resonances are likely to occur in transmission. On the other hand, if more channels are generated in the hybridized region than in the leads, transmissions may exhibit antiresonances.

To understand the mechanism and characteristics of antiresonances in transmissions through our hybrid nanotubes, we consider a simple transport model (see Fig. 2), where a single incident channel is split into two channels in the hybridized region, and then these two channels are recombined into one channel. In this model, we derive a formula for the total transmission T using a symmetric 3×3 S matrix with time reversal symmetry, which describes incoming and outgoing waves at junctions,

$$\begin{pmatrix} O_0 \\ O_1 \\ O_2 \end{pmatrix} = \begin{pmatrix} r_0 & t_1 & t_2 \\ t_1 & r_1 & r_{12} \\ t_2 & r_{12} & r_2 \end{pmatrix} \begin{pmatrix} I_0 \\ I_1 \\ I_2 \end{pmatrix}, \tag{5}$$

where r_0 is the reflection coefficient of an incident channel, r_1 and r_2 are the reflection coefficients of two channels in the

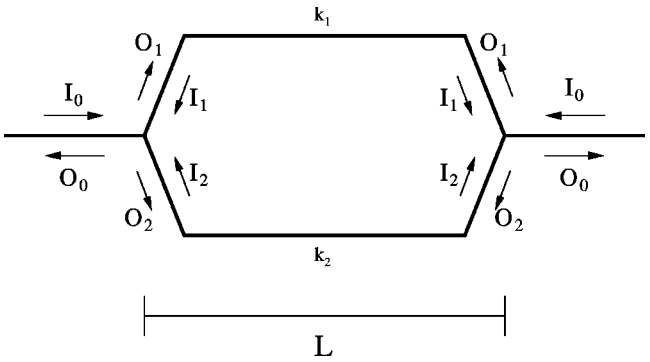

FIG. 2. The schematic diagram of the channel flow in the hybridized region. An incident channel is split into two channels at one junction, and then these are recombined into one channel at the other junction. Here I_i and O_i denote incoming and outgoing waves, respectively, at each junction.

hybridized region, t_1 and t_2 are the transmission coefficients of an incident channel into channels 1 and 2, respectively, and r_{12} is the reflection from channel 1 to 2 and vice versa. From Eq. (5), the transmission matrices at the separation ($\tilde{t}_S$) and recombination ($\tilde{t}_R$) junctions and the reflection matrix (**R**) for electrons moving in the hybridized region are expressed as

$$\tilde{t}_S=\begin{pmatrix} t_1 \\ t_2 \end{pmatrix}, \quad \tilde{t}_R=(t_1 \;\; t_2), \quad \mathbf{R}=\begin{pmatrix} r_1 & r_{12} \\ r_{12} & r_2 \end{pmatrix}.$$

To describe wave propagation in the hybridized region, we represent the propagation matrix (**P**),

$$\mathbf{P}=\begin{pmatrix} e^{ik_1L} & 0 \\ 0 & e^{ik_2L} \end{pmatrix},$$

where k_1 and k_2 are the wave vectors of channels 1 and 2, respectively, in a hybridized region with length L. Considering multiple reflections in the hybridized region, we can write the transmission of an incident channel as[12]

$$T=|t|^2=|\tilde{t}_R\mathbf{M}\mathbf{P}\tilde{t}_S|^2, \tag{6}$$

where $\mathbf{M}=\mathbf{I}+\mathbf{PRPR}+(\mathbf{PRPR})^2+\cdots$. After some algebra, Eq. (6) is rewritten as

$$\begin{aligned} T=\frac{1}{|\gamma|^2}|&t_1^2e^{ik_1L}(1-r_2^2e^{2ik_2L}-r_{12}^2e^{i(k_1+k_2)L}) \\ &+t_2^2e^{ik_2L}(1-r_1^2e^{2ik_1L}-r_{12}^2e^{i(k_1+k_2)L}) \\ &+2r_{12}t_1t_2e^{i(k_1+k_2)L}(r_1e^{ik_1L}+r_2e^{ik_2L})|^2, \end{aligned} \tag{7}$$

where

$$\begin{aligned} \gamma=&[1-r_1e^{ik_1L}-r_2e^{ik_2L}+(r_1r_2-r_{12}^2)e^{i(k_1+k_2)L}] \\ &\times[1+r_1e^{ik_1L}+r_2e^{ik_2L}+(r_1r_2-r_{12}^2)e^{i(k_1+k_2)L}]. \end{aligned}$$

The unitarity of the S matrix can be satisfied by introducing six independent parameters defined as

$$\begin{aligned} r_0&=re^{i(\psi+\theta)}, \\ t_1&=\sqrt{(1-r^2)\epsilon}e^{i[(\phi_1+\psi)/2+\theta]}, \\ t_2&=\sqrt{(1-r^2)(1-\epsilon)}e^{i[(\phi_2+\psi)/2+\theta]}, \\ r_1&=-[(1-\epsilon)+\epsilon r]e^{i(\phi_1+\theta)}, \\ r_2&=-[\epsilon+(1-\epsilon)r]e^{i(\phi_2+\theta)}, \\ r_{12}&=(1-r)\sqrt{\epsilon(1-\epsilon)}e^{i[(\phi_1+\phi_2)/2+\theta]}. \end{aligned} \tag{8}$$

In Eq. (8), only two parameters r and ϵ are physically meaningful; $|r|$ is the reflection coefficient of an incident channel and ϵ represents the coupling of an incident channel with channel 1 in the hybridized region, satisfying the conditions $|r|<1$ and $0<\epsilon<1$. From Eqs. (6) and (8), we derive a simple formula for the total transmission,

$$T=\frac{(1-r^2)^2}{|\alpha|^2|\beta|^2}\frac{\sin^2(\eta/2+\theta_0)}{\sin^2(\eta/2+\theta_0+\Delta)+\Gamma_0^2}, \tag{9}$$

where $\theta_0=\theta+\delta$, $\delta=\arg(r')$, $\Delta=\arg(\beta/\alpha)$, $\alpha=1+re^{i\eta}$, $\beta=1+re^{i\phi}$, $\phi=(k_2-k_1)L+\phi_2-\phi_1$, and $\eta=(k_1+k_2)L+\phi_1+\phi_2$. Here the linewidth Γ_0 is related to r by

$$\Gamma_0=\left|\frac{1-|r'^2\beta/\alpha|}{2r'\beta/\alpha}\right|, \tag{10}$$

where $r'=(1-\epsilon)e^{-i\phi/2}+\epsilon e^{i\phi/2}$.

For $r\neq 0$, transmission barriers exist between the lead and hybridized regions, and then r is regarded as the background reflection,[22] which causes the Fano resonance.[23] In this case, since Δ is generally not equal to zero, the Fano resonance has an asymmetric line shape, and the resonance peak becomes sharper as r goes to 1. On the other hand, for $r=0$, the transmission has the Breit-Wigner antiresonance form[24] with the linewidth $\Gamma_0[=(1-|r'|^2)/(2|r'|)]$,

$$T=\frac{\sin^2(\eta/2+\theta_0)}{\sin^2(\eta/2+\theta_0)+\Gamma_0^2}. \tag{11}$$

In actual hybrid nanotube systems, the parameters such as Γ, α, and β depend on k_1, k_2, ϵ, and r. Nevertheless, the line shapes of resonances and antiresonances are mainly determined by r. In multichannel transport, we also expect antiresonances in transmission, if the number of channels increases in the hybridized region, compared with the incident channels. In this case, line shapes are also determined by the background reflections.

IV. RESULTS AND DISCUSSION

A. SWNT encapsulating a capsule

In this section, we calculate the total transmissions through the (10,10) tubes containing finite-sized (5,5) nanotube capsules, with and without mirror symmetries, and investigate the effect of mirror symmetries on the antiresonance line shape. For the consistency of our calculations, we

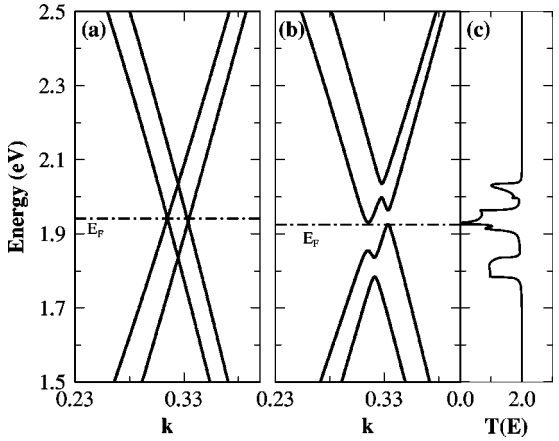

FIG. 3. The band structure of infinite (5,5)-(10,10) double-wall nanotubes, where the inner tube is aligned (a) to retain mirror symmetries in cross section and (b) breaking mirror symmetries. In (b), the inner tube is rotated by 3° about the tube axis. (c) The total transmission through the (10,10) tube containing a semi-infinite capped (5,5) tube with broken mirror symmetries.

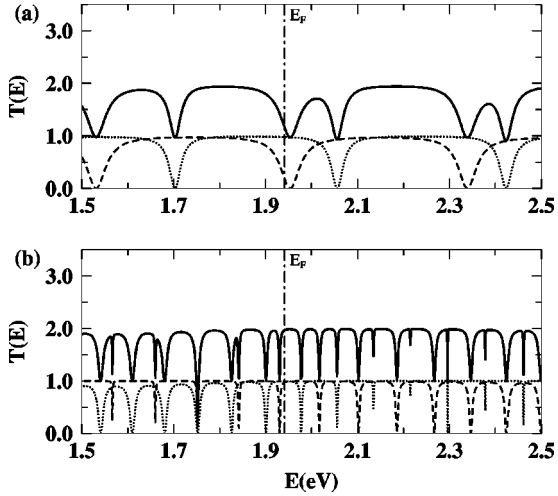

FIG. 4. The total (solid) and eigenchannel (dashed and dotted) transmissions through the (10,10) tubes where the (5,5) capsules are aligned with mirror symmetries. The dashed and dotted lines denote the transmissions through the π and π^* channels, respectively. The capsules contain (a) 11 and (b) 60 unit cells of the perfect (5,5) tube.

calculate the band structure of the double-wall (5,5)-(10,10) nanotube (see Fig. 3), and find good agreement with previous theoretical calculations.[25,26] In armchair nanotubes, two linear bands near the Fermi level are characterized by π and π^*, which have even and odd parities, respectively, under mirror symmetry operations. Thus, if mirror symmetries are maintained, the double-wall nanotube keeps the characteristics of the (5,5) and (10,10) tubes without a mixing of the π and π^* states, exhibiting linear parallel bands, as shown in Fig. 3(a). In the double-wall tube without mirror symmetries, the π and π^* states are mixed, and pseudogaps are created at energies where the linear bands are crossed [see Fig. 3(b)].

To get insight into the reflection of incident channels at the beginning of the hybridized region, we also examine the transmission through the (10,10) tube containing the semi-infinite (5,5) tube with a cap, which is shown in Fig. 1(c). For energies near the Fermi level, we find that transmissions are almost equal to 2 with retained mirror symmetries, indicating that incident channels are negligibly reflected. If mirror symmetries are broken, transmissions are greatly reduced near the pseudogaps [see Fig. 3(c)], with significant reflections of incident waves.

For the (10,10) tube containing a finite-sized (5,5) capsule that retains mirror symmetries, the total and eigenchannel transmissions are drawn in Fig. 4. In this system, since both the π and π^* channels are eigenchannels, the single-channel model can be used for deriving the total transmission; the incident π (π^*) channel is connected with the π (π^*) channels of the (5,5) capsule and (10,10) tube in the hybridized region. As in the case of a semi-infinite (5,5) tube, incident channels are negligibly reflected due to mirror symmetries, i.e., $r \simeq 0$. Since the linear bands of the (5,5) and (10,10) tubes are parallel, the difference between k_1 and k_2 is independent of energy, where k_1 and k_2 denote the wave vectors of the two channels with energy E in the hybridized region. Then, the total transmission in Eq. (9) is reduced to the form

$$T = \frac{\sin^2(k_1 L + \varphi)}{\sin^2(k_1 L + \varphi) + \Gamma_0^2}, \tag{12}$$

where $\varphi = \theta + \phi/2 + \phi_1$ and L is the capsule length. In Eq. (12), antiresonances occur at energies $E = E_n$, where n is an integer and k_1 satisfies the resonance condition $k_1 L + \varphi = n\pi$. Then, the total transmission has a Breit-Winger-type symmetric line shape such as

$$T \simeq \frac{(E - E_n)^2}{(E - E_n)^2 + \Gamma^2}, \tag{13}$$

where $\Gamma = \Gamma_0 a/L$. From the resonance condition, we get the energy difference between two neighboring antiresonances, $\Delta E \propto \Delta k = \pi/L$, indicating that ΔE tends to decrease as L increases. Moreover, the linewidth Γ also decreases with increasing L. In fact, we find that each eigenchannel exhibits periodic antiresonance dips with symmetric line shapes, as shown in Fig. 4, and both the linewidth and period decrease with increasing L.

When the number of channels in the hybridized region is larger than that of the incident channels, antiresonances exist, regardless of the presence of mirror symmetries. However, if mirror symmetries are broken, since the π and π^* channels are coupled in the hybridized region, the incident channels are reflected near the pseudogaps, i.e., background reflections exist. Since the coupling of the π and π^* channels depends on energy, the linewidth depends on energy, too. In this case, antiresonances exhibit asymmetric line shapes, as shown in Fig. 5.[27] We analyze the antiresonance dips near the Fermi level, where the π and π^* channels are strongly mixed due to band crossings. In the two-channel transport model, eigenchannel transmissions can be obtained by diagonalizing the transmission matrix

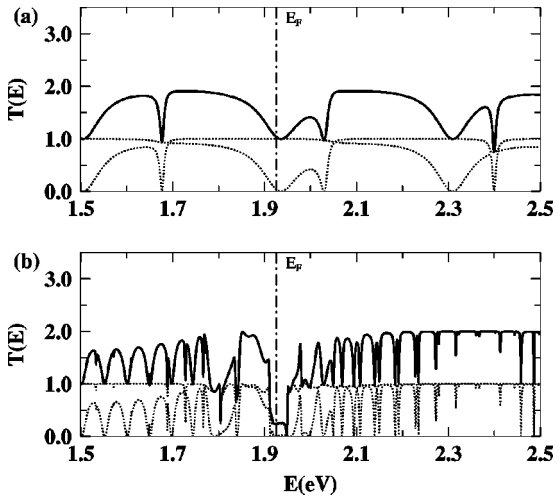

FIG. 5. The total (solid) and eigenchannel (dotted) transmissions through the (10,10) tubes where the (5,5) capsules are rotated by 3° about the outer tube axis, with broken mirror symmetries. Two dotted lines represent more ($T_>$) and less ($T_<$) transmissive channels. The capsules contain (a) 11 and (b) 110 unit cells of the perfect (5,5) tube.

$$\tilde{T}=\begin{pmatrix} T_1 & T_{12} \\ T_{12} & T_2 \end{pmatrix}, \tag{14}$$

where T_1 and T_2 denote the transmissions through channels 1 and 2, respectively, in the hybridized region, and T_{12} is the transmission from channel 1 to channel 2. The eigenchannel transmissions in Eqs. (3) and (4) are expressed as $T_{\gtrless}=[T_1+T_2\pm[(T_1-T_2)^2+4T_{12}^2]^{1/2}]/2$. If T_{12} is not zero, $T_>$ and $T_<$ exhibit very different behavior near the Fermi level, as illustrated in Fig. 5; $T_>$ almost equals 1, while $T_<$ has a pair of antiresonances.

B. SWNT encapsulating a chain of C_{60} molecules

For an isolated C_{60} molecule, the lowest unoccupied molecular orbital (LUMO) states are triply degenerate and characterized by $m=-1$, 0, and $+1$, where m denotes the angular momentum quantum number.[28–30] The π-like state with $m=0$ has even parity under mirror symmetry operations in cross sections perpendicular to the fivefold symmetry axis. When a C_{60} molecule is contained in the (10,10) tube, the LUMO states lie just above the Fermi level of the (10,10) tube, while the highest occupied molecular orbital state of C_{60} is located at 1.4 eV below the Fermi level, as shown in Fig. 6(a). In this case, if both mirror and rotational symmetries are maintained, only the $m=0$ state is coupled to the π state of the (10,10) tube for energies near the Fermi level, resulting in a single antiresonance, i.e., $T(E)$ decreases by one unit. However, the total transmission is not affected for other energies having two channels of π and π^*, as shown in Figs. 7 and 8(a). Here we focus on energies near the Fermi level where the LUMO states interact with incident channels. If two C_{60} molecules are aligned with the van der Waals spacing in the (10,10) tube, two antiresonances are expected due to two off-phase bound states[31] split by interactions between the two molecules. However, since this intermolecule interaction is very weak, the energy splitting is much smaller than the linewidths. Thus, the pair-annihilation effect[32] occurs for the two antiresonances located close to each other, resulting in a reduced single antiresonance dip, as shown in Fig. 8(a).

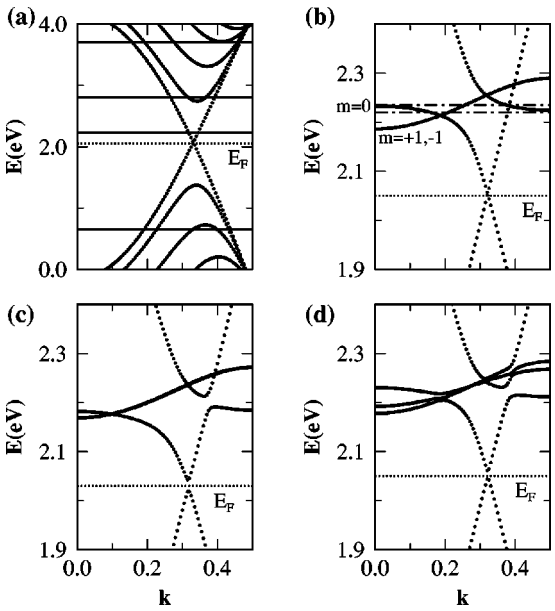

FIG. 6. (a) The energy levels (solid flat lines) of an isolated C_{60} molecule and the band structure of a (10,10) tube. The band structure of the (10,10) tubes where C_{60} molecules are aligned periodically (b) with both mirror and rotational symmetries, (c) with only rotational symmetries, and (d) without symmetries. In (c), each C_{60} molecule is rotated by 3° about the outer tube axis, and in (d) it is further rotated by 5° about the one axis perpendicular to the tube axis and then by 3° about the other perpendicular axis.

As the number of C_{60} molecules increases in the hybridized region, we still expect antiresonances because of the coupling of incident channels with the molecular states of C_{60}'s. To understand the transmission behavior, we calculate the band structure [see Fig. 6(b)] for an infinite chain of C_{60} molecules aligned in the (10,10) tube with both mirror and rotational symmetries. The $m=0$ state of C_{60} is also found to

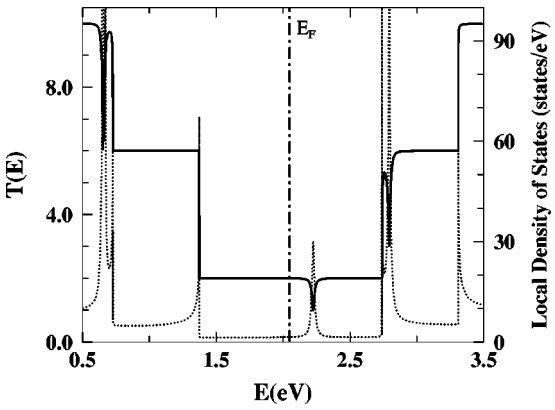

FIG. 7. The total transmission (solid) and local density of states (dotted) for the (10,10) tube containing a single C_{60} molecule.

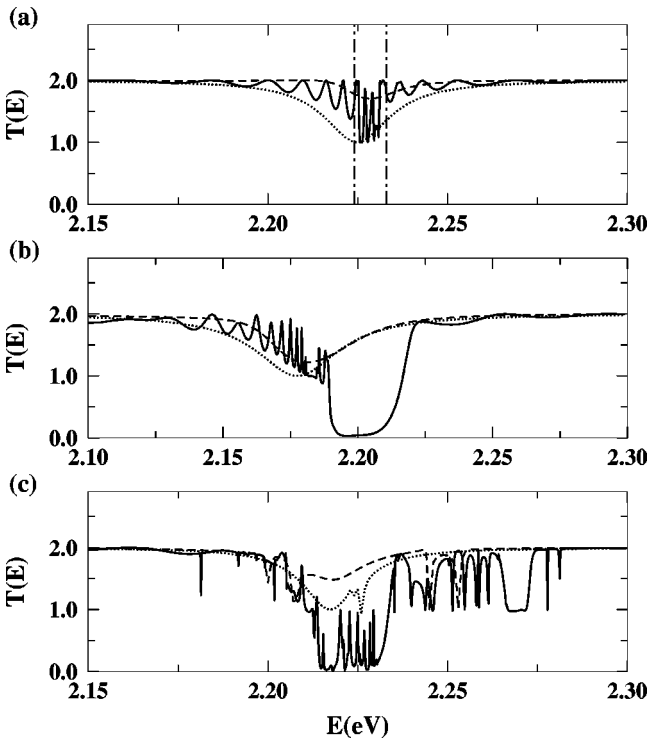

FIG. 8. The total transmissions through (10,10) tubes containing a finite number of C_{60} molecules, (a) with both mirror and rotational symmetries, (b) with only rotational symmetries, and (c) without symmetries. Dotted, dashed, and solid lines represent the total transmissions for one, two, and 22 C_{60} molecules, respectively, inside the (10,10) tube.

be coupled to the π state, while the $m=-1$ and $+1$ states are not affected. We find that two transport channels, which result from the coupling of the $m=0$ and π states, exist in a narrow range of energies 2.224–2.233 eV. For the (10,10) tube with a long chain of C_{60}'s, in this energy range, antiresonances may occur in the π eigenchannel because the number of channels in the hybridized region is larger than that in the leads. However, in this case, because the two additional channels in the hybridized region are generated from the $m=0$ state rather than the π state, the incident π channel is strongly reflected, i.e., $r\sim 1$. Thus, we find that resonance peaks, instead of antiresonances, are accumulated in the total transmission for a very long chain of 22 C_{60} molecules, as shown in Fig. 8(a). Moreover, the group velocity of the π band decreases very rapidly as the incident energy approaches the coupled region of 2.224–2.233 eV, while it is almost constant for the perfect tube. The oscillatory behavior of the total transmission results from the difference of the group velocities in the lead and hybridized regions.

When C_{60} molecules are rotated about the tube axis, only the mirror symmetries are broken. Then, the $m=0$ state interacts with both the π and π^* states of the (10,10) tube, creating a pseudogap, as shown in Fig. 6(c). In fact, this pseudogap results from the mixing of π and π^* and behaves as a transmission barrier. Although the $m=-1$ and $+1$ states are in the gap region, they do not affect the transmission through the outer tube. For a very few C_{60} molecules, because the pseudogap is negligible, transmissions are similar to those obtained by keeping the mirror symmetries. For the long chain of 22 C_{60} molecules, we find a transmission gap due to the pseudogap, as shown in Fig. 8(b). In this case, however, antiresonances do not appear clearly in the long C_{60} chain, because the energy range where the number of channels is larger than that of the incident channels is extremely narrow.

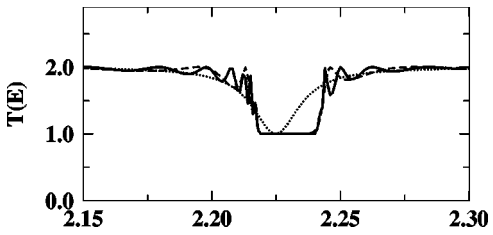

FIG. 9. The total transmissions through the (10,10) tubes where C_{60} molecules are aligned with the intermolecule spacing of 2 nm, retaining both mirror and rotational symmetries. Dotted, dashed, and solid lines represent the total transmissions for one, five, and 12 C_{60} molecules, respectively, inside the (10,10) tube.

When rotational symmetries are further broken by rotating C_{60} molecules about an arbitrary axis, all the states ($m=-1,0,+1$) interact with the incident π and π^* channels of the (10,10) tube, as illustrated in Fig. 6(d). For a single C_{60} molecule, we find three antiresonances which are caused by the $m=-1$, 0, and $+1$ states. For the long chain, resonance peaks appear in the transmission gap due to the coupling of incident channels with the $m=-1$ and $+1$ states [see Fig. 8(c)]. In addition, we find antiresonances and transmission drops by one unit outside the gap region.

We examine the effect of intermolecule interactions on transmission in the C_{60} chain. As the separation of neighboring molecules is much larger than the van der Waals spacing, individual molecules can be regarded as independent resonators, and give rise to antiresonances. In this case, the transport behavior can be explained by analogy with the serial stub structure.[33] We find a flat region with $T(E)=1$ and oscillatory behavior in transmission, which are caused by the interference effect of the antiresonances generated by molecules, as shown in Fig. 9. Such features become clearer as the number of C_{60} molecules increases. Finally, if C_{60} molecules are randomly oriented inside the (10,10) tube, all the symmetries will be broken. Since this hybrid system does not have periodicity, transmission gaps will not appear. Then antiresonances are expected to be accumulated, and interactions between these antiresonances may give various structures in transmission.

V. SUMMARY

In summary, we have investigated the transport properties of hybrid (10,10) carbon nanotubes encapsulating a (5,5) nanotube capsule and a chain of C_{60} molecules. In these hybrid systems, we find that the alignment of the inner structures plays an important role in the transport behavior through the outer tubes. The coupling of transport channels

with the bound states of the inner structures is very sensitive to the symmetry of the hybrid tubes. Thus, we find rich structures in transmission, such as antiresonances, Fano resonances, and transmission gaps. To understand the mechanism for antiresonances and resonances, we have derived a transmission formula where one incident channel is coupled to two channels in the hybridized region. From the transmission formula, we find that line shapes depend on the reflection of incident channels and the wave vectors of propagating channels in the hybridized region. For the (10,10) tube containing a finite-sized (5,5) capsule, when the capsule maintains mirror symmetries, antiresonances have symmetric line shapes, while asymmetric line shapes occur in the absence of mirror symmetries. On the other hand, for the (10,10) tube containing a chain of C_{60} molecules, transmissions are mostly affected for energies where the lowest unoccupied state of C_{60} is located just above the Fermi level. When both mirror and rotational symmetries are maintained, antiresonance dips are found in the π channel transmission for a few C_{60} molecules. As the chain length increases, since the incident π channel is strongly reflected, resonance peaks appear instead of antiresonances. When only mirror symmetries are broken, a transmission gap occurs due to the mixing of π and π^*. If all the symmetries are broken, all the lowest unoccupied states of C_{60} interact with the incident channel, resulting in resonance peaks in the transmission gap.

ACKNOWLEDGMENTS

We thank Dr. H.-W. Lee for helpful discussions. This work was supported by the QSRC at Dongguk University.

[1] S. Iijima, Nature (London) **354**, 56 (1991).
[2] C. Dekker, Phys. Today **52** (5), 22 (1999).
[3] S.J. Tans, M.H. Devoret, H. Dai, A. Thess, R.E. Smalley, L.J. Geerligs, and C. Dekker, Nature (London) **386**, 474 (1997).
[4] M. Bockrath, D.H. Cobden, P.L. McEuen, N.G. Chopra, A. Zettle, A. Thess, and R.E. Smalley, Science **275**, 1922 (1997).
[5] A. Bezryadin, A.R.M. Verschueren, S.J. Tans, and C. Dekker, Phys. Rev. Lett. **80**, 4036 (1998).
[6] L.C. Venema, J.W.G. Wilder, J.W. Janssen, S.J. Tans, H.L.J.T. Tuinstra, L.P. Kouwenhoven, and C. Dekker, Science **283**, 52 (1999).
[7] A. Rubio, D. Sánchez-Portal, E. Artacho, P. Ordejón, and J.M. Soler, Phys. Rev. Lett. **82**, 3520 (1999).
[8] R.A. Jishi, J. Bragin, and L. Lou, Phys. Rev. B **59**, 9862 (1999).
[9] V. Meunier, P. Senet, and Ph. Lambin, Phys. Rev. B **60**, 7792 (1999).
[10] L. Chico, M.P. López Sancho, and M.C. Muñoz, Phys. Rev. Lett. **81**, 1278 (1998).
[11] M.P. Anantram and T.R. Govindan, Phys. Rev. B **61**, 5020 (2000).
[12] H.-S. Sim, C.-J. Park, and K.J. Chang, Phys. Rev. B **63**, 073402 (2001).
[13] B.W. Smith, M. Monthioux, and D.E. Luzzi, Nature (London) **396**, 323 (1998); Chem. Phys. Lett. **315**, 31 (1999).
[14] J. Sloan, R.E. Dunin-Borkowski, J.L. Hutchison, K.S. Coleman, V.C. Williams, J.B. Claridge, A.P.E. York, C. Xu, S.R. Bailey, G. Brown, S. Friedrichs, and M.L.H. Green, Chem. Phys. Lett. **316**, 91 (2000).
[15] Z. Shao, W. Porod, and C.S. Lent, Phys. Rev. B **49**, 7453 (1994).
[16] Other structural changes such as longitudinal displacement and radial displacement of the capsule are not considered because their effects can be replaced by rotating the capsule about the tube axis. Only whether mirror symmetries are preserved or not is important in the coupling of the outer tube and capsule.
[17] M. Büttiker, Y. Imry, R. Landauer, and S. Pinhas, Phys. Rev. B **31**, 6207 (1985).
[18] Y. Meir and N.S. Wingreen, Phys. Rev. Lett. **68**, 2512 (1992).
[19] M.S. Tang, C.Z. Wang, C.T. Chan, and K.M. Ho, Phys. Rev. B **53**, 979 (1996).
[20] M.P. López Sancho, J.M. López Sancho, and J. Rubio, J. Phys. F: Met. Phys. **14**, 1205 (1984); **15**, 851 (1985).
[21] M. Büttiker, IBM J. Res. Dev. **32**, 63 (1988); in *Electronic Properties of Multilayers and Low-Dimensional Semiconductor Structure*, edited by J.M. Chamberlain *et al.* (Plenum, New York, 1990).
[22] J.U. Nöckel and A.D. Stone, Phys. Rev. B **50**, 17 415 (1994).
[23] U. Fano, Phys. Rev. **124**, 1866 (1961).
[24] G. Breit and E. Wigner, Phys. Rev. **49**, 519 (1936).
[25] Y.K. Kwon and D. Tománek, Phys. Rev. B **58**, R16 001 (1998).
[26] S. Sanvito, Y.K. Kwon, D. Tománek, and C.J. Lambert, Phys. Rev. Lett. **84**, 1974 (2000).
[27] The asymmetric line shape is evident as the capsule length increases, because the pseudogaps are clearer for longer capsules.
[28] R.C. Haddon, L.E. Brus, and K. Raghavachari, Chem. Phys. Lett. **125**, 459 (1986).
[29] S. Saito and A. Oshiyama, Phys. Rev. Lett. **66**, 2637 (1991).
[30] E. Manousakis, Phys. Rev. B **44**, R10 991 (1991).
[31] H.-W. Lee, Phys. Rev. Lett. **82**, 2358 (1999).
[32] H.-W. Lee and C.S. Kim, J. Korean Phys. Soc. **37**, 137 (2000); Phys. Rev. B **63**, 075306 (2001).
[33] P. Signha Deo and A.M. Jayannavar, Phys. Rev. B **50**, 11 629 (1994).